Temperature-Insensitive Near-Infrared Spectroscopic Measurement of Glucose in Aqueous Solutions

KEVIN H. HAZEN, MARK A. ARNOLD,* and GARY W. SMALL

Department of Chemistry, Iowa City, Iowa 52242 (K.H.H., M.A.A.); and Center for Intelligent Chemical Instrumentation, Department of Chemistry, Clippinger Laboratories, Ohio University, Athens, Ohio 45701-2979 (G.W.S.)

A digital Fourier filter is combined with partial least-squares (PLS) regression to generate a calibration model for glucose that is insensitive to sample temperature. This model is initially created by using spectra collected over the 5000 to 4000 cm^{-1} spectral range with samples maintained at 37°C. The analytical utility of the model is evaluated by judging the ability to determine glucose concentrations from a set of prediction spectra. Absorption spectra in this prediction set are obtained by ratioing single-beam spectra collected from solutions at temperatures ranging from 32 to 41°C to reference spectra collected at 37°C. The temperature sensitivity of the underlying water absorption bands creates large baseline variations in prediction spectra that are effectively eliminated by the Fourier filtering step. The best model provides a mean standard error of prediction across temperatures of 0.14 mM (2.52 mg/dL). The benefits of the Fourier filtering step are established, and critical experimental parameters, such as number of PLS factors, mean and standard deviation for the Gaussian shaped Fourier filter, and spectral range, are considered.

Index Headings: **Near-infrared measurement of glucose; Temperature-insensitive NIR measurements in aqueous matrices; Digital filtering; PLS regression.**

INTRODUCTION

Temperature is a critical parameter for near-infrared (NIR) spectroscopic analysis of aqueous-based samples. The major water absorption bands are centered at approximately 3800, 5200, and 6900 cm^{-1}, but the exact positions of these bands are temperature-sensitive. Changes in temperature alter the extent of hydrogen bonding, which causes significant shifts in the band positions. These bands shift to higher frequencies at higher temperatures. The large water content of most clinical samples necessitates precise control of sample temperature to ensure accurate results.[1-3]

Noninvasive clinical measurements by NIR spectroscopy are particularly prone to temperature-induced errors because noninvasive measurement configurations do not permit rigorous temperature control. Although mechanical devices to control the temperature at the measurement site can be envisioned, such devices are subject to many practical limitations. Ideally, the analytical measurement is independent of sample temperature, which, for NIR analyses, means the calibration model must be insensitive to baseline variations that can be several orders of magnitude larger than the size of the analyte absorption bands.

This paper details a temperature-insensitive spectral processing scheme for measuring clinically relevant levels of glucose in an aqueous matrix by NIR spectroscopy. A digital Fourier filter is used in combination with partial least-squares (PLS) regression to provide a calibration model that is insensitive to temperature over the range from 32 to 41°C. The validity of this approach has been verified by using a calibration model generated with spectra collected at 37°C to predict glucose concentrations from spectra collected at the other temperatures. In all cases, absorbance spectra are computed by using background spectra collected at 37°C. The mean standard error of prediction (SEP) across all temperatures tested is 0.14 mM (2.52 mg/dL) even though, in some cases, baseline deviations are orders of magnitude greater than the glucose absorption bands.

EXPERIMENTAL

Apparatus and Reagents. Spectra were collected with a Nicolet Model 740 Fourier transform (FT) spectrometer (Nicolet Instruments, Madison, WI). The source was a 150-W tungsten–halogen lamp configured with a back reflecting mirror. A calcium fluoride beamsplitter and a cryogenically cooled indium antimonide (InSb) detector were used. The incident light was restricted to the 5000–4000 cm^{-1} (2.00–2.50 μm) range by using a multilayer optical interference filter (Barr Associates, Westford, MA) with 72% transmittance at 4400 cm^{-1}. The Jacquinot aperture was maintained at a setting of 70 for both samples and buffer solutions. All sample and background spectra were collected with an instrument gain setting of one. Samples were placed in a 1-mm-pathlength rectangular cell composed of Infrasil quartz (Wilmad Glass Co., Buena, NJ). Temperatures were maintained at the desired value (±0.1°C) by placing the sample cell in an aluminum-jacketed cell holder in conjunction with a VWR Model 1140 refrigerated temperature bath (VWR Scientific, Chicago, IL). Temperatures were monitored with a copper-constantan thermocouple probe (Omega Inc., Stamford, CT) placed directly in the sample. An Omega Model 670 digital meter was used to read out temperatures.

All glucose samples were prepared by dissolving dried reagent-grade glucose in a pH 7.3 working buffer. This buffer was composed of 0.1 M phosphate and 0.483 g/L 5-fluorouracil. Buffer solutions were prepared with type I, reagent-grade water obtained from a three-stage Milli-Q water purification system.

Procedures. Spectra were collected as double-sided interferograms with 16,384 points based on 256 coadded scans. Interferograms were triangularly apodized and Fourier transformed to produce single-beam spectra with 1.9-cm^{-1} point spacing. Mertz phase correction was applied to the spectra with the phase array used based on

Received 3 September 1993; revision received 30 December 1993.
* Author to whom correspondence should be sent.

0003-7028/94/4804-0477$2.00/0

in den beiden Wassertransmissionsfenstern von ca. 6800-5400 cm^{-1} und 4750-4200 cm
während im "wasserfreien" Gebiet oberhalb von ca. 7200 cm^{-1} bei der Schichtdicke 1 mm n
sehr schwache Oberton- bzw. Kombinationsbanden der Glucose auftreten (vgl. Abb.3.6
Abb.5.14b zeigt das Extinktionsspektrum einer lipämischen Plasmaprobe mit pathologisc
erhöhter Blutfett-Konzentration, die im sichtbaren Spektralbereich trüb ist (Probenröhrchen m
ϕ=10 mm undurchsichtig). Die diffuse Streuung nimmt in lipämischen Proben für kürzere
Wellenlängen zu, wodurch sich beim NIR-Transmissionsverfahren ein in der Wellenzahl $\tilde{\upsilon}$ in
guter Näherung linearer Anstieg der Extinktion einstellt. Von den 126 Plasmaproben waren
zwei stark lipämisch und wurden als Ausreißer aus allen NIR-Kalibrationen entfernt. Hierdurch
verminderte sich der Populationsmittelwert (M=124) für die Triglyceride auf $\bar{c}_{Pop}$=158.1 mg/dL,
während die Mittelwerte der übrigen Substrate (Tab.5.1) nahezu unverändert blieben.

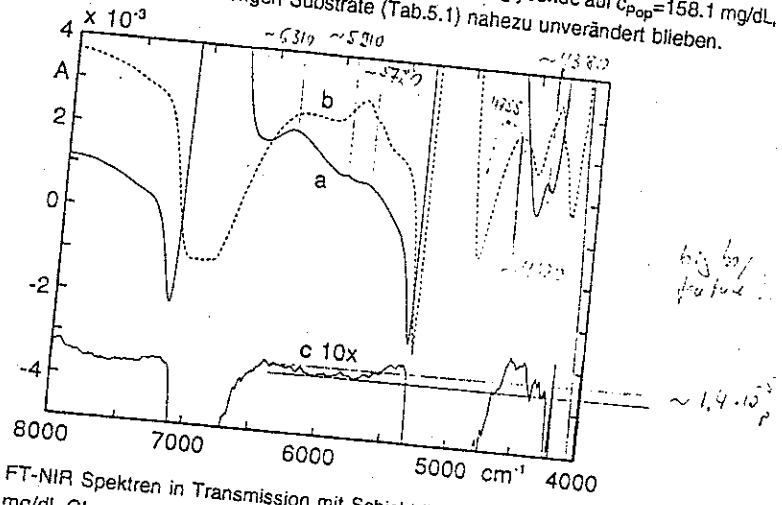

Abb.5.15: FT-NIR Spektren in Transmission mit Schichtdicke 1 mm: (a) Extinktion von 800 mg/dL Glucose in wässriger Lösung; (b) Korrelationsspektrum der Glucose für die 124 Blutplasmen ($\bar{c}_{Pop}$=206.4 mg/dL); (c) Extinktionsrauschen aus zwei Wasserreferenzen (mit Offset und Vergrößerung).

In Abb.5.15 ist die ungünstige Ausgangssituation für die Glucosekalibration im NIR dargestellt. Die stärksten NIR-Banden bei ca. 6350 cm^{-1} und 4400 cm^{-1} (Abb.5.15a) erzeugen Extinktionen in der Größenordnung $1 \cdot 10^{-6}$ AU/(mg/dL), so daß die Signale beim physiologischen Normalwert von 100 mg/dL zum Rauschen der Extinktion (c) vergleichbar sind. Im Korrelationsspektrum der Glucose (b) sind die Signale als Bandenschultern nur angedeutet erkennbar. Die beiden starken Korrelationsbanden im Wasserfenster 4750-4200 cm^{-1} entstehen durch die positive Korrelation der Glucose zu anderen Blutsubstraten, ha[illegible]ächlich Eiweiß und Cholesterin (vgl. Tab.5.2). Das extrem schlecht konditionierte M[illegible]oblem der Glucosebestimmung im NIR ist in Abb.5.15 gut dokumentiert.

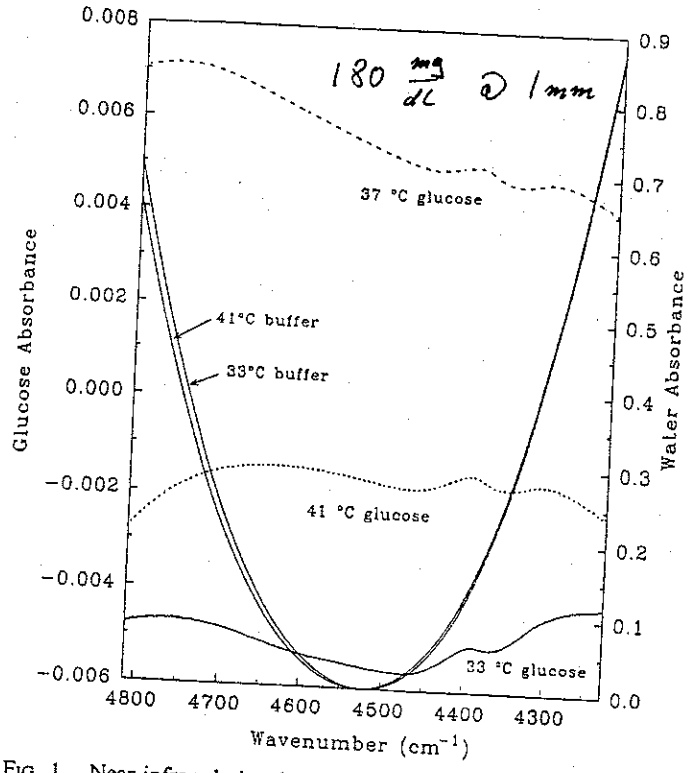

FIG. 1. Near-infrared absorbance spectra for water (solid lines) and glucose at the indicated temperatures.

200 points on each side of the interferogram centerburst. The resulting single-beam spectra were transferred for further processing to the Vax 6400 computer system at the Gerard P. Weeg Computing Center at the University of Iowa. All software was implemented in FORTRAN 77. Subroutines for Fourier filtering and multiple linear regression computations were obtained from the IMSL software package (IMSL, Inc., Houston, TX).

A series of spectra was collected for calibration purposes. The solution temperature was maintained at 37°C for this data set. Triplicate spectra were collected for each of 46 unique glucose standard solutions that ranged in concentration from 1.25 to 19.66 mM. Triplicate spectra were collected sequentially without removing a given sample from the spectrometer. From the resulting 138 single-beam spectra, 80 were selected at random for further analysis. Background spectra were collected from glucose-free buffer solutions maintained at 37°C. A new background spectrum was collected after every third glucose standard solution.

A separate series of spectra was collected for prediction purposes. For this data set, triplicate single-beam spectra were collected for six unique glucose standard solutions at each temperature from 32 to 41°C at 1°C increments. Once again, triplicate spectra were collected sequentially without removing the solution from the spectrometer. This protocol provided 18 spectra at each of ten temperatures for a total of 180 spectra. Two spectra were subsequently discarded because of obvious spectral anomalies. The glucose concentrations used for this prediction data set were unique compared to those used for the calibration data set. Specifically, 3.09, 5.80, 9.01, 12.08, 15.03, and 17.98 mM glucose standards were used for generating the prediction data set.

All spectra for a given temperature were collected sequentially during a single data collection session. Within each data collection session, the glucose concentrations were taken randomly. The order of temperatures was random. Spectra for all temperatures were collected over a six-day period, except for the 34°C spectra, which were collected one week later.

RESULTS AND DISCUSSION

Glucose and Water Absorption Band Positions. Positions of the three major glucose absorbance bands in the spectral region between 5000 and 4000 cm^{-1} are not sensitive to changes in temperature over the range from 33 to 41°C. Figure 1 includes absorbance spectra for a 10 mM glucose solution collected at 33, 37, and 41°C. In each spectrum, the effect of water has been diminished by using a background spectrum collected at the same temperature as the sample. The strong absorbance of water is evident by the large variation in baseline. This baseline variation is characterized by y-axis offsets and differences in the slope and shape of the baseline. Nevertheless, the three characteristic glucose absorption bands centered at ~4750, 4400, and 4300 cm^{-1} are clearly visible in each spectrum. The positions, sizes, and shapes of the 4400- and 4300-cm^{-1} bands appear to remain constant over this temperature range. In fact, positions of the 4400- and 4300-cm^{-1} bands have been noted to remain constant up to 62°C.[4] The integrity of the 4750-cm^{-1} band is compromised considerably at 33°C because of a dramatic decrease in optical throughput caused by shifts in the underlying water bands. Nevertheless, the position of the 4750-cm^{-1} band also appears to remain constant, at least between 37 and 41°C. At temperatures closer to 37°C, where this glucose band is less distorted by changing water absorbances, the 4750-cm^{-1} band position appears constant.

The insensitivity of these bands to temperature corroborates assignment of these spectral features to combination bands associated with C–H stretching vibrational transitions.[5,6] Vibrational characteristics of any O–H groups on the glucose molecule would be affected by hydrogen bonding with water, and, hence, overtone and combination bands associated with O–H vibrational transitions would be temperature-sensitive. The carbon–hydrogen stretching vibrations likely correspond to the equatorial C–H bonds in the pyranose ring and/or the CH_2 plane deformation at C-6 in nonglycosidic glucose.

In comparison, absorption bands associated with water shift to higher frequencies at higher temperatures. Two water absorption spectra are provided in Fig. 1 for the spectral range from 4811 to 4227 cm^{-1}. These water spectra were obtained by ratioing buffer single-beam spectra to an air background spectrum. This figure reveals that the glucose bands are located between the two large water absorption bands centered at 5200 and 3800 cm^{-1}. Although only a portion of these water bands is present in this figure, the effect of temperature is evident. Both bands shift to higher frequencies at higher temperatures, but the magnitude of shift is significantly greater for the 5200-cm^{-1} band. The differences in absorbance at 4750, 4400, and 4300 cm^{-1} for the water spectra in Fig. 1 are 0.02075, 0.00697, and 0.00809, respectively. These changes are

considerably greater than those for the glucose absorbance bands.

Temperature-dependent shifts in the positions of the water absorbance bands generate large baseline variations in absorbance spectra when the temperatures of the glucose sample solutions do not match those of the reference solution. Examples of this phenomenon are illustrated in the absorbance spectra presented in Fig. 2A. These spectra correspond to 5.98, 12.08 and 17.98 mM glucose solutions collected at 33, 37, and 41°C with a buffer reference spectrum collected at 37°C. This figure clearly shows that baseline variations are much larger than the glucose absorbance bands. In fact, the glucose bands are difficult to see with the absorbance scale needed to encompass the entire span of baseline variation. When the temperature of the sample is lower than that of the reference solution, positive baseline deviations are observed at high frequencies and negative baseline deviations are obtained at low frequencies. The baseline deviations change in the opposite direction when the sample temperature is greater than the reference solution temperature. Such baseline deviations are consistent with the shifting of the water absorbance bands to higher frequencies at higher temperatures. In addition, the magnitudes of these baseline deviations are considerably larger at the high-frequency side because of the greater temperature sensitivity displayed by the 5200-cm^{-1} water band (see Fig. 1).

The spectra in Fig. 2A also demonstrate significant baseline variations for absorbance spectra collected at the same temperature. Such baseline shifts appear as simple offsets and are caused by slight variations in instrument alignment and source intensities during the normal course of data collection.

This analysis of the temperature sensitivity of the glucose and water spectral band positions suggests that the 4400-cm^{-1} glucose band should be the least affected by changes in temperature for two reasons. First, this band is located near the minimum between the water bands, which results in relatively high optical throughputs and large signal-to-noise ratios. Second, the water absorbance spectrum should be least sensitive to temperature variations in this spectral range, thereby resulting in relatively smaller baseline variations in the vicinity of the 4400-cm^{-1} glucose band. Correspondingly, the band at 4750 cm^{-1} should be the most affected by temperature variations because of the high temperature sensitivity of water in this spectral region. The 4300-cm^{-1} band will also be largely affected because it is located high on the shoulder of the 3800-cm^{-1} water band, which results in relatively low optical throughput and poor signal-to-noise ratios.

PLS Regression Analysis. As noted elsewhere,[7] the spectral range and number of factors used in the PLS algorithm are critical parameters when a calibration model of this type is being generated. The following four spectral ranges were examined in this work: 4850–4220, 4811–4457, 4457–4354, and 4354–4227 cm^{-1}. The first encompasses all three of the glucose bands, while the second, third, and fourth ranges selectively focus on each glucose band individually.

The optimum number of PLS factors has been determined for each spectral range by computing the mean SEP for the prediction data set across all temperatures (32–41°C) as a function of the number of PLS factors.

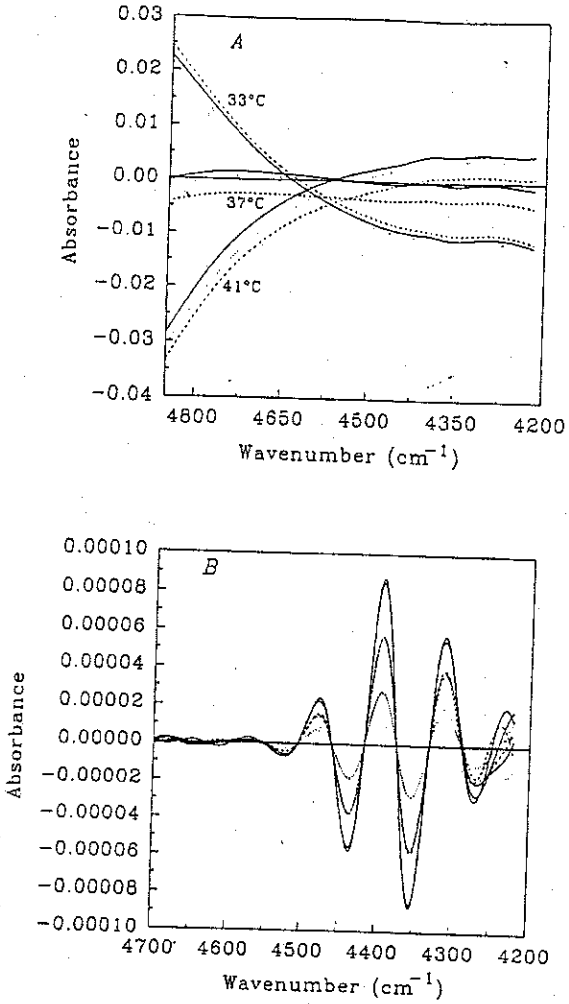

FIG. 2. Glucose absorbance spectra for 5.98 (dotted line), 12.08 (dashed line), and 17.98 mM (solid line) glucose for 33, 37, and 41°C spectra (A) before filtering and (B) after digital Fourier filtering.

Calibration models were computed by considering from 1 to 20 PLS factors. In each case, the calibration model was constructed from only 37°C data. The number of factors corresponding to the minimum mean SEP was taken as the optimum. Figure 3A shows a surface that represents the effect of the number of factors on the SEP as a function of temperature for the 4850–4220 cm^{-1} spectral range. The effect of the number of factors on the standard error of calibration (SEC) is also plotted in Fig. 3A for comparison. Both the SEC and SEP drop sharply as the first factors account for the large water-induced baseline deviations. As expected, however, the SEC continues to decrease as the number of factors is increased and more of the spectral variation in the calibration data set is incorporated into the model. The SEP, on the other hand, drops to a minimum value and then increases as the system is over-modeled by too many factors. For this spectral range, the minimum mean SEP across all temperatures is 0.44 mM (7.9 mg/dL) when nine factors are used. The corresponding SEC is 0.15 mM (2.7 mg/dL) with nine PLS factors.

The surface in Fig. 3A indicates a systematic variation in the SEP across temperatures. Generally, the SEP is larger for temperatures further away from 37°C. For ex-

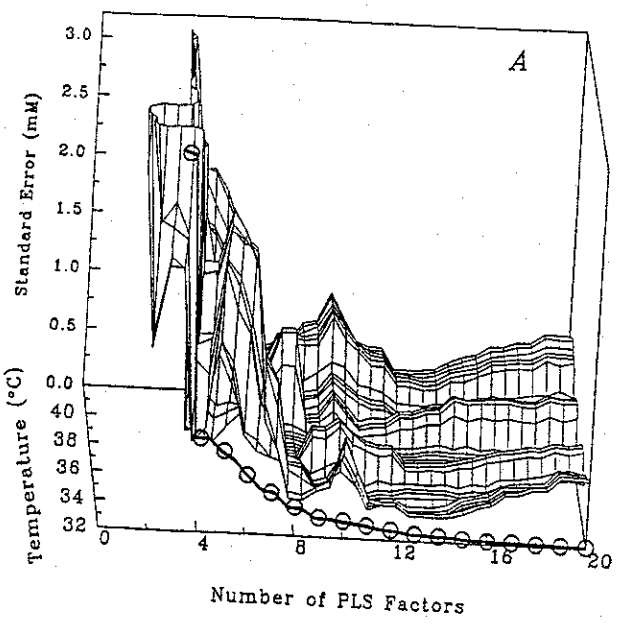

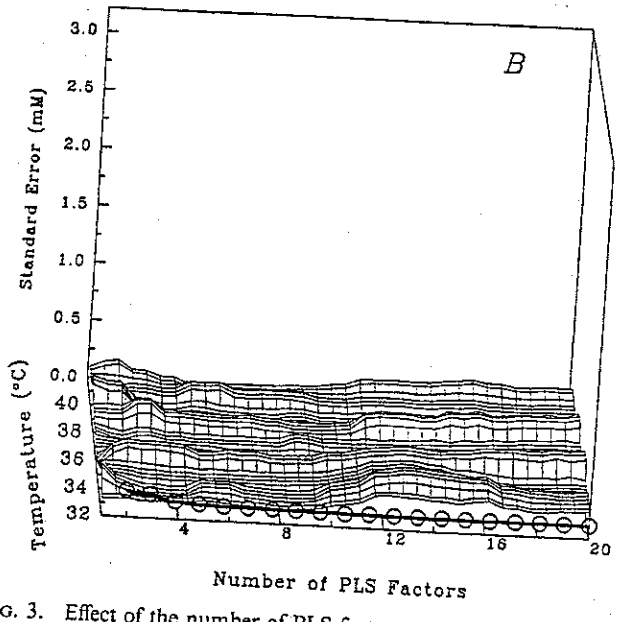

FIG. 3. Effect of the number of PLS factors on the SEC (open circle) and SEP (mesh) for spectra collected from 32 to 41°C over the 4850–4220 cm^{-1} region, (**A**) using PLS and (**B**) using PLS after digital Fourier filtering.

ample, SEPs are 0.309, 0.241, and 0.729 mM for 33, 37, and 41°C, respectively, when nine PLS factors are used.

Similar results have been found for the other spectral ranges when analyzed by PLS alone. Table I summarizes the major features of the best calibration model obtained with each of the four spectral ranges. Fewer factors were needed with the narrower spectral regions. The lowest mean SEP across all temperatures was obtained with the spectral range that included only the 4400-cm^{-1} glucose band. This result confirms the same finding from our other studies[1,7,8] and demonstrates the predicted utility of the 4400-cm^{-1} band because of its position relative to the water bands. Furthermore, our analysis of the temperature-sensitive band positions concludes that the 4750- and 4300-cm^{-1} bands should be strongly influenced by temperature, and, indeed, the corresponding SEPs indicate that these two bands are significantly inferior in comparison to the 4400-cm^{-1} band.

TABLE I. Results from best calibration models.

Spectral range (cm^{-1})	PLS			Fourier filter and PLS				
	PLS factors	SEC[a] (mM)	SEP[b] (mM)	PLS factors	Gaussian filter Mean	Gaussian filter Std dev	SEC[a] (mM)	SEP[b] (mM)
4811–4457	4	2.25	2.28	9	0.0185	0.0022	0.13	0.15
4457–4354	5	0.23	0.25	1	0.0286	0.0051	0.16	0.18
4354–4227	5	0.89	2.39	10	0.0254	0.0034	0.14	0.17
4850–4220	9	0.15	0.44	8	0.0264	0.0049	0.11	0.14

[a] Computed with only 37°C data.
[b] Computed over all temperatures (32–41°C).

Fourier Filter Parameters. Digital Fourier filtering has been used effectively to enhance the signal-to-noise ratio for NIR measurements of glucose in aqueous-based solutions.[1,7,8] Here, Fourier filtering is used as a preprocessing tool to isolate the glucose absorption bands relative to other spectral features, such as baseline variations. This filtering procedure is implemented by first computing the Fourier transformation of a raw absorbance spectrum, then multiplying this transformed spectrum by a Gaussian function, and finally computing the inverse Fourier transformation to return to the original data domain of an absorbance spectrum.[1] The success of this filtering step depends on the mean position and standard deviation, or width, of the Gaussian function. These parameters determine the spectral band shapes that pass through the Fourier filter. Ideally, parameters can be established so that glucose information selectively passes through the filter while unwanted spectral features, such as noise and baseline variation, are blocked.

The optimal mean position and standard deviation width for the Gaussian-shaped filter response function were determined for each of the four spectral ranges by a slightly different procedure than has been described before.[7] Parameters for the Gaussian were determined for a given number of PLS factors by using only spectra collected at 37°C. Ten of the 80 spectra in the calibration data set were used to construct a "monitoring set" that was used as a pseudo-prediction data set.[8] These ten spectra corresponded to six unique glucose concentrations that span the whole concentration range. All replicate spectra for these concentrations were also removed from the calibration set and added to the monitoring set. Initially, the number of PLS factors was set, and then values for the mean position and standard deviation width were varied systematically. For each combination of position and width, all spectra in the calibration and monitoring data sets were subjected to the Fourier filter. A PLS regression calibration model was generated by using the calibration data set and the set number of factors. Finally a value was computed for a response function which was defined as the reciprocal of the sum of the mean square error (MSE), taken from the calibration set, and the mean square prediction error (MSPE), taken from the moni-

toring set. This process was repeated for each pair of mean position and standard deviation width, which typically involved between 3000 and 5000 unique calibration models. The ideal combination of mean position and standard deviation width for the given number of PLS factors was identified as the values that provided the largest response function value or the lowest combination of calibration and prediction errors.

The selected surface response function [1/(MSE + MSPE)] incorporates both the quality of calibration and the prediction into the optimization procedure. We have found that inclusion of calibration quality is critical when a limited number of spectra are available. With only six glucose concentrations available for the monitoring set, Fourier filter parameters can be obtained that result in calibration models with excellent prediction ability but poor calibration quality. The system is easily over-modeled by using prediction ability exclusively with a limited number of observations. Under these conditions, a response function that incorporates both MSE and MSPE is critical.

An iterative approach was used to determine the optimum number of PLS factors. First, the Fourier filter parameters found to be optimal by the procedure described above were used to generate a PLS calibration model for a given number of PLS factors. Each model was used to predict glucose concentrations from spectra in the prediction data set (i.e., spectra collected at temperatures from 32 to 41°C with background spectra collected at 37°C). A mean SEP was computed from all spectra in the prediction data set. The mean SEP was obtained as a function of the number of PLS factors used in the calibration model. If the number of PLS factors corresponding to lowest mean SEP differed from the number of factors used to optimize the Gaussian function parameters for the Fourier filter, the Gaussian parameter optimization scheme was repeated with the new "best" number of factors. This entire process was repeated until the number of factors used to generate the filter parameters matched the number yielding the minimum mean SEP across temperatures.

A typical surface map is illustrated in Fig. 4 for the 4850–4220 cm^{-1} spectral range with eight PLS factors. A rather broad feature is observed with a maximum value for the response function given at a mean position of 0.0264 f (digital frequency units) and a standard deviation width of 0.0049 f. The broad shape of this feature indicates that precise values for mean and standard deviation are not critical for acceptable model performance. This same finding has been observed when calibration models for glucose in undiluted plasma matrices are constructed.[8]

The effectiveness of the Fourier filtering process to reduce spectral variation is demonstrated by the filtered spectra plotted in Fig. 2B. This figure shows the same spectra originally presented in Fig. 2A after processing with the Fourier filter presented in the preceding paragraph. Baseline variation is essentially eliminated by filtering the spectra. Indeed, filtered spectra collected at different temperatures overlap for the same concentration of glucose. The derivative appearance of these filtered spectra has been observed in all our work and is explained elsewhere.[8] Although the filter parameters used to generate the spectra in Fig. 2B incorporated the entire spectral

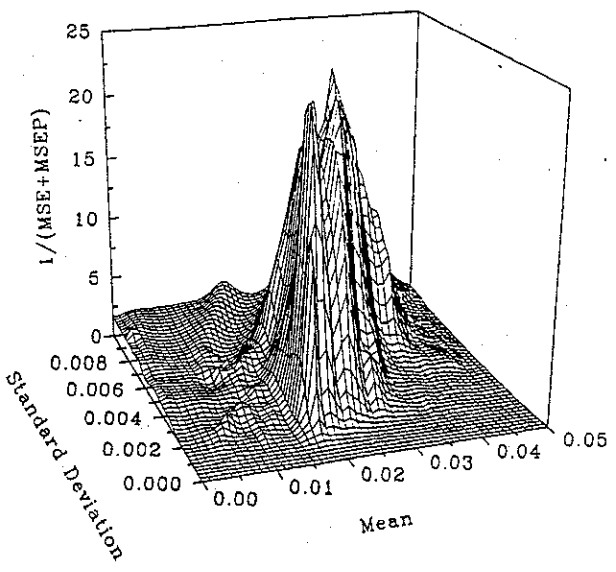

FIG. 4. Filter response curve for varying means and standard deviations of the Gaussian filter over the 4850–4220 cm^{-1} spectral region.

range from 4850 to 4220 cm^{-1}, the glucose information is clearly localized to a much smaller range from 4500 to 4250 cm^{-1}. The optimization procedure has generated a Fourier filter that extracts information predominantly from the 4400- and 4300-cm^{-1} glucose bands.

Compared to calibration models based on PLS regression alone, incorporation of a Fourier filter preprocessing step significantly reduces the number of PLS factors required to generate the ideal calibration model. Figure 3B presents a surface map that shows SEP values for different numbers of PLS factors (1–20) as a function of temperature. The corresponding SEC for each number of factors is also plotted in this figure. Because digital filtering minimizes the large baseline variations, the first few PLS factors yield much smaller SEPs in comparison to those generated by the PLS method applied without filtering (see Fig. 3A). The SEP and SEC approach the same value and vary only slightly after the first few factors. In addition, there is essentially no variation in the SEP as a function of temperature. Most importantly, incorporation of a Fourier filtering step results in significantly lower SEPs at all temperatures, in comparison to processing by PLS regression alone.

Calibration Models. Calibration models have been constructed for each of the previously described spectral ranges by using only PLS and by combining PLS with Fourier filtering. Table I summarizes the details of these calibration models in terms of the optimum number of factors, SEC, and mean SEP across temperatures. For models with digital filtering, the optimum filter parameters of mean position and standard deviation width are provided. The key parameter to consider is the SEP, which indicates the ability of the model to accurately predict glucose concentrations from spectra collected at different temperatures. It is important to recognize that these models have been generated without information regarding temperature variation included in the calibration data set. Moreover, the effect of shifting water bands is accentuated in this experiment by ratioing spectra collected at one temperature to a reference spectrum collected at 37°C.

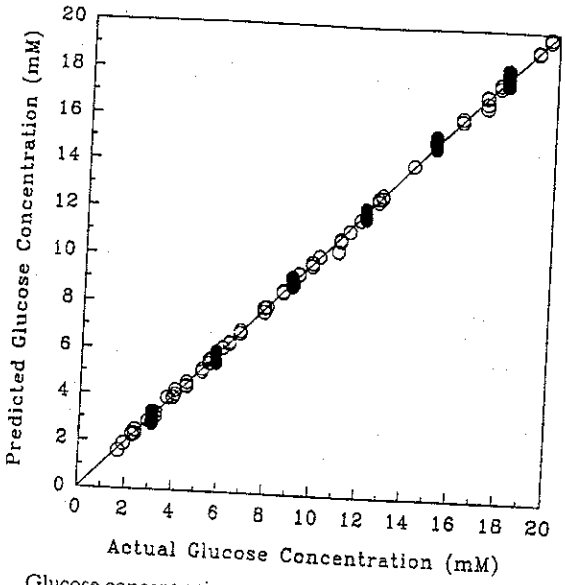

FIG. 5. Glucose concentration correlation plot comparing results from the NIR calibration model with the known glucose concentrations. Open circles represent calibration data, and filled circles correspond to prediction data. The calibration model used a spectral range from 4850 to 4220 cm^{-1}, a PLS regression with eight factors, and a Gaussian-shaped Fourier filter defined by a mean of 0.0264 f and a standard deviation of 0.0049 f.

For all ranges tested, superior calibration models are generated with the digital filtering step included in the processing scheme. Results from the calibration model based on the 4850–4220 cm^{-1} range with Fourier filtering and eight PLS factors are presented in Fig. 5. This concentration correlation graph shows glucose concentrations predicted by the model plotted against actual glucose concentrations. The open and closed circles represent the calibration and prediction data, respectively, where predictions correspond to the group of 178 spectra at different temperatures. The SEC is 0.11 mM (1.98 mg/dL) and the SEP is 0.14 mM (2.5 mg/dL). Tight clustering of both the calibration and prediction data about the unity line and the low standard error values demonstrate the analytical utility of this model. The Fourier filtering step provides a 3.1-fold improvement in the ability to predict, in comparison to the model generated over this same spectral range without Fourier filtering.

Sensitivity to temperature is best examined by assessing the accuracy of predictions from spectra collected at different temperatures. Surface maps showing the percent error of prediction as functions of temperature and glucose concentration are presented in Fig. 6, where Fig. 6A and 6B correspond to results without and with filtering, respectively. Relative prediction errors are generally larger without filtering, especially at the lower glucose concentrations. Moreover, the prediction errors increase as the temperature difference increases between sample and reference spectra. Figure 6A indicates that standard errors are particularly high for all concentrations at the higher temperatures. For the Fourier filter/PLS system, on the other hand, there is no indication of a temperature dependency on the percent error. Although relative prediction errors are slightly higher at low concentrations, which is expected for an absorbance measurement, this effect is constant across temperatures.

As indicated by the values listed in Table I, the quality

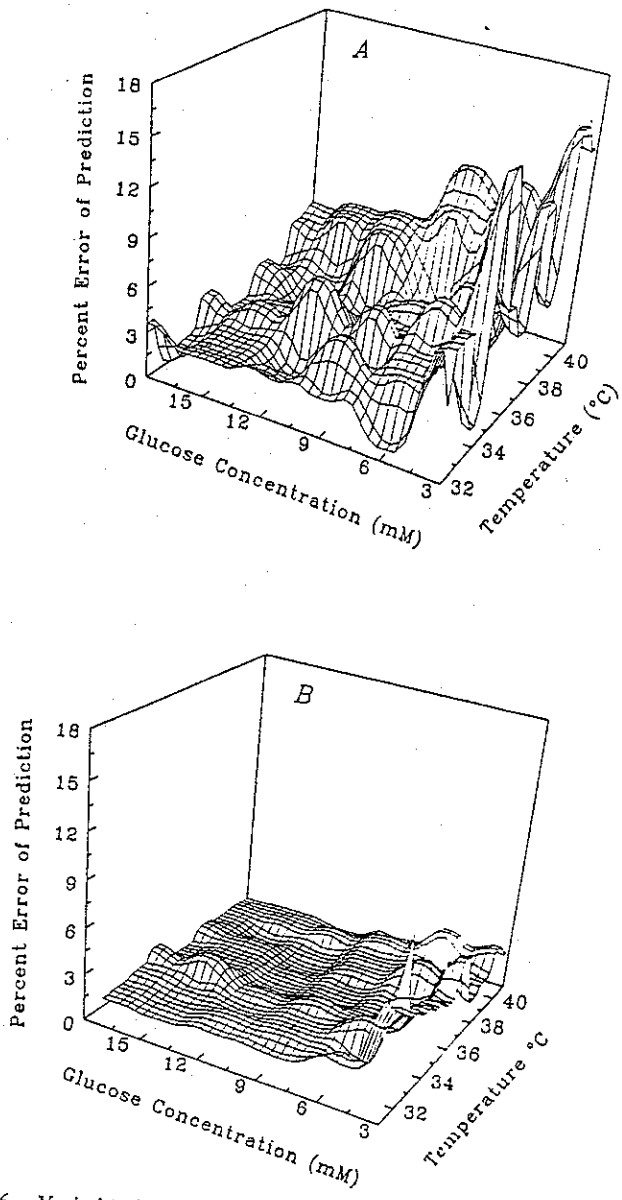

FIG. 6. Variation in percent error of prediction over the 4850–4220 cm^{-1} region for 3.09 to 17.98 mM glucose spectra from 32 to 41°C, using (A) PLS alone and (B) PLS after digital Fourier filtering.

of the calibration model is most affected by the spectral range when a digital filter is not used in the data processing scheme. Without filtering, the lowest SEP is obtained by using the range corresponding solely to the 4400-cm^{-1} glucose band. The ability to predict is unacceptable when ranges corresponding to either the 4750- or 4300-cm^{-1} glucose bands are used exclusively. These findings strongly indicate that the 4400-cm^{-1} glucose band provides the most reliable information. As mentioned above, the utility of this band is likely related to the relative insensitivity of this spectral region to temperature-induced spectral variations caused by water.

With digital filtering, however, standard errors of calibration and prediction are essentially the same for all spectral ranges tested. The range isolating the 4400-cm^{-1} band requires only one PLS factor for the best SEP. More factors are needed for the other ranges. The best mean and standard deviation are similar for the whole range

and the ranges corresponding to the 4400- and 4300-cm^{-1} bands. These bands have similar shapes (see Fig. 1), which accounts for the similarity in filter parameters. The 4750-cm^{-1} band possesses a considerably different shape, which mandates different filter parameters. The filter parameters found optimal for the 4850–4220 cm^{-1} range indicate that the calibration model relies mainly on the spectral information located within the 4400- and 4300-cm^{-1} bands.

CONCLUSIONS

A spectral processing scheme involving a Fourier filtering step followed by PLS regression analysis provides a calibration model that is insensitive to sample temperature over the range from 32 to 41°C. Digital Fourier filtering selectively passes the desired spectral features, which effectively reduces the adverse effects caused by large baseline variations. Overall, unwanted baseline deviations are eliminated. It should be stressed that this method is not exclusive to the question of measuring glucose, but is general in nature and can be applied to the NIR analysis of any aqueous based sample.

Although this work focuses on the issue of temperature variation, the results are promising for the potential to reduce chemical interferences by digital filtering techniques. Changes in concentration of a strongly absorbing interfering species would effectively alter the spectral baseline. Results in this paper indicate that the effects of such an interference can be reduced by identifying the appropriate filter parameters that selectively pass glucose information. The key requirement for success is a significant difference in the spectral band shapes between glucose and potential interferences, such as protein and triglycerides. The larger the differences in spectral band shapes, the more likely these compounds can be discriminated in digital frequency space and, thus, be effectively separated. It remains to be seen whether digital filtering will be adequate to permit valid calibration models under conditions of varying concentrations of numerous, strongly absorbing interferences. In an effort to help address these questions, this methodology is currently being explored as a method for enhancing the measurement of glucose in matrices characterized by changing levels of protein and triglycerides. In addition, the combination of digital filtering and PLS regression is being evaluated for the measurement of glucose in whole blood matrices.

ACKNOWLEDGMENT

This work was supported by grants from the National Institutes of Health (RR04583 and DK45126).

1. M. A. Arnold and G. W. Small, Anal. Chem. **62**, 1457 (1990).
2. B. Bauer and T. A. Floyd, Anal. Chim. Acta **197**, 295 (1987).
3. J. Hall and A. Pollard, Clin. Chem. **38**, 1623 (1992).
4. T. B. Colin, Ph.D. Dissertation, University of Iowa, Iowa City (1991).
5. E. Stark, Proc. SPIE 8th Internat. Conf. Fourier Transform Spectrosc. **1575**, 70 (1991).
6. I. M. Mills, Proc SPIE 8th Internat. Conf. Fourier Transform Spectrosc. **1575**, 96 (1991).
7. L. A. Marquardt, M. A. Arnold, and G. W. Small, Anal. Chem. **65**, 3271 (1993).
8. G. W. Small, M. A. Arnold, and L. A. Marquardt, Anal. Chem. **65**, 3279 (1993).